

Novel Aspects of Hard Diffraction in QCD

Stanley J. Brodsky

Stanford Linear Accelerator Center, Stanford University, Stanford, CA, 94309

Initial- and final-state interactions from gluon-exchange, normally neglected in the parton model have a profound effect in QCD hard-scattering reactions, leading to leading-twist single-spin asymmetries, diffractive deep inelastic scattering, diffractive hard hadronic reactions, and nuclear shadowing and antishadowing—leading-twist physics not incorporated in the light-front wavefunctions of the target computed in isolation. I also discuss the use of diffraction to materialize the Fock states of a hadronic projectile and test QCD color transparency.

1 Diffractive Deep Inelastic Scattering

A remarkable feature of deep inelastic lepton-proton scattering at HERA is that approximately 10% events are diffractive^{1,2}: the target proton remains intact, and there is a large rapidity gap between the proton and the other hadrons in the final state. These diffractive deep inelastic scattering (DDIS) events can be understood most simply from the perspective of the color-dipole model: the $q\bar{q}$ Fock state of the high-energy virtual photon diffractively dissociates into a diffractive dijet system. The exchange of multiple gluons between the color dipole of the $q\bar{q}$ and the quarks of the target proton neutralizes the color separation and leads to the diffractive final state. The same multiple gluon exchange also controls diffractive vector meson electroproduction at large photon virtuality.³ This observation presents a paradox: if one chooses the conventional parton model frame where the photon light-front momentum is negative $q^+ = q^0 + q^z < 0$, the virtual photon interacts with a quark constituent with light-cone momentum fraction $x = k^+/p^+ = x_{bj}$. Furthermore, the gauge link associated with the struck quark (the Wilson line) becomes unity in light-cone gauge $A^+ = 0$. Thus the struck “current” quark apparently experiences no final-state interactions. Since the light-front wavefunctions $\psi_n(x_i, k_{\perp i})$ of a stable hadron are real, it appears impossible to generate the required imaginary phase associated with pomeron exchange, let alone large rapidity gaps.

This paradox was resolved by Paul Hoyer, Nils Marchal, Stephane Peigne, Francesco Sannino and myself.⁴ Consider the case where the virtual photon interacts with a strange quark—the $s\bar{s}$ pair is assumed to be produced in the target by gluon splitting. In the case of Feynman gauge, the struck s quark continues to interact in the final state via gluon exchange as described by the Wilson line. The final-state interactions occur at a light-cone time $\Delta\tau \simeq 1/\nu$ shortly after the virtual photon interacts with the struck quark. When one integrates over the nearly-on-shell intermediate state, the amplitude acquires an imaginary part. Thus the rescattering of the quark produces a separated color-singlet $s\bar{s}$ and an imaginary phase. In the case of the light-cone gauge $A^+ = \eta \cdot A = 0$, one must also consider the final-state interactions of the (unstruck) \bar{s} quark. The gluon propagator in light-cone gauge $d_{LC}^{\mu\nu}(k) = (i/k^2 + i\epsilon) [-g^{\mu\nu} + (\eta^\mu k^\nu + k^\mu \eta^\nu / \eta \cdot k)]$ is singular at $k^+ = \eta \cdot k = 0$. The momentum of the exchanged gluon k^+ is of $\mathcal{O}(1/\nu)$; thus rescattering contributes at leading twist even in light-cone gauge. The net result is gauge invariant and is identical to the color dipole model calculation. The calculation of the rescattering effects on DIS in Feynman and light-cone gauge through three loops is given in detail for an Abelian model in the references.⁴ The result shows that the rescattering corrections reduce the magnitude of the DIS cross section in analogy to nuclear shadowing.

A new understanding of the role of final-state interactions in deep inelastic scattering has thus emerged. The multiple scattering of the struck parton via instantaneous interactions in the target generates dominantly imaginary diffractive amplitudes, giving rise to an effective “hard pomeron” exchange. The presence of a rapidity gap between the target and diffractive system requires that the target remnant emerges in a color-singlet state; this is made possible

in any gauge by the soft rescattering. The resulting diffractive contributions leave the target intact and do not resolve its quark structure; thus there are contributions to the DIS structure functions which cannot be interpreted as parton probabilities⁴; the leading-twist contribution to DIS from rescattering of a quark in the target is a coherent effect which is not included in the light-front wave functions computed in isolation. One can augment the light-front wave functions with a gauge link corresponding to an external field created by the virtual photon $q\bar{q}$ pair current.^{5,6} Such a gauge link is process dependent⁷, so the resulting augmented LFWFs are not universal.^{4,5,8} We also note that the shadowing of nuclear structure functions is due to the destructive interference between multi-nucleon amplitudes involving diffractive DIS and on-shell intermediate states with a complex phase. In contrast, the wave function of a stable target is strictly real since it does not have on-energy-shell intermediate state configurations. The physics of rescattering and shadowing is thus not included in the nuclear light-front wave functions, and a probabilistic interpretation of the nuclear DIS cross section is precluded.

Rikard Enberg, Paul Hoyer, Gunnar Ingelman and I⁹ have shown that the quark structure function of the effective hard pomeron has the same form as the quark contribution of the gluon structure function. The hard pomeron is not an intrinsic part of the proton; rather it must be considered as a dynamical effect of the lepton-proton interaction. Our QCD-based picture also applies to diffraction in hadron-initiated processes. The rescattering is different in virtual photon- and hadron-induced processes due to the different color environment, which accounts for the observed non-universality of diffractive parton distributions. This framework also provides a theoretical basis for the phenomenologically successful Soft Color Interaction (SCI) model¹⁰ which includes rescattering effects and thus generates a variety of final states with rapidity gaps.

2 Single-Spin Asymmetries from Final-State Interactions

Among the most interesting polarization effects are single-spin azimuthal asymmetries in semi-inclusive deep inelastic scattering, representing the correlation of the spin of the proton target and the virtual photon to hadron production plane: $\vec{S}_p \cdot \vec{q} \times \vec{p}_H$. Such asymmetries are time-reversal odd, but they can arise in QCD through phase differences in different spin amplitudes. In fact, final-state interactions from gluon exchange between the outgoing quarks and the target spectator system lead to single-spin asymmetries in semi-inclusive deep inelastic lepton-proton scattering which are not power-law suppressed at large photon virtuality Q^2 at fixed x_{bj} .¹¹ In contrast to the SSAs arising from transversity and the Collins fragmentation function, the fragmentation of the quark into hadrons is not necessary; one predicts a correlation with the production plane of the quark jet itself. Physically, the final-state interaction phase arises as the infrared-finite difference of QCD Coulomb phases for hadron wave functions with differing orbital angular momentum. The same proton matrix element which determines the spin-orbit correlation $\vec{S} \cdot \vec{L}$ also produces the anomalous magnetic moment of the proton, the Pauli form factor, and the generalized parton distribution E which is measured in deeply virtual Compton scattering. Thus the contribution of each quark current to the SSA is proportional to the contribution $\kappa_{q/p}$ of that quark to the proton target's anomalous magnetic moment $\kappa_p = \sum_q e_q \kappa_{q/p}$.^{11,12} The HERMES collaboration has recently measured the SSA in pion electroproduction using transverse target polarization.¹³ The Sivers and Collins effects can be separated using planar correlations; both contributions are observed to contribute, with values not in disagreement with theory expectations.^{13,14} A related analysis also predicts that the initial-state interactions from gluon exchange between the incoming quark and the target spectator system lead to leading-twist single-spin asymmetries in the Drell-Yan process $H_1 H_2^\dagger \rightarrow \ell^+ \ell^- X$.^{7,15} The SSA in the Drell-Yan process is the same as that obtained in SIDIS, with the appropriate identification of variables, but with the opposite sign. Initial-state interactions also lead to a $\cos 2\phi$ planar correlation in unpolarized Drell-Yan reactions.¹⁶ There is no Sivers effect in charged-current

reactions since the W only couples to left-handed quarks.¹⁷

3 Diffraction Dissociation as a Tool to Resolve Hadron Substructure

Diffraction multi-jet production in heavy nuclei provides a novel way to resolve the shape of light-front Fock state wave functions and test color transparency.¹⁸ For example, consider the reaction^{19,20} $\pi A \rightarrow \text{Jet}_1 + \text{Jet}_2 + A'$ at high energy where the nucleus A' is left intact in its ground state. The transverse momenta of the jets balance so that $\vec{k}_{\perp 1} + \vec{k}_{\perp 2} = \vec{q}_{\perp} < R^{-1} A$. Because of color transparency, the valence wave function of the pion with small impact separation will penetrate the nucleus with minimal interactions, diffracting into jet pairs.¹⁹ The $x_1 = x$, $x_2 = 1 - x$ dependence of the di-jet distributions will thus reflect the shape of the pion valence light-cone wave function in x ; similarly, the $\vec{k}_{\perp 1} - \vec{k}_{\perp 2}$ relative transverse momenta of the jets gives key information on the second transverse momentum derivative of the underlying shape of the valence pion wavefunction.^{20,21} The diffractive nuclear amplitude extrapolated to $t = 0$ should be linear in nuclear number A if color transparency is correct. The integrated diffractive rate will then scale as $A^2/R_A^2 \sim A^{4/3}$. This is in fact what has been observed by the E791 collaboration at FermiLab for 500 GeV incident pions on nuclear targets.²² The measured momentum fraction distribution of the jets is found to be approximately consistent with the shape of the pion asymptotic distribution amplitude.^{23,24,25} $\phi_{\pi}^{\text{asympt}}(x) = \sqrt{3}f_{\pi}x(1-x)$.²⁶ Remarkably this is also the prediction of AdS/CFT duality for the light-front wavefunctions of the pion in conformal QCD.²⁷

The concept of high energy diffractive dissociation can be generalized to provide a tool to materialize the individual Fock states of a hadron, photon, or nuclear projectile; *e.g.*, the diffractive or Coulomb dissociation of a high energy proton $pA \rightarrow qq\bar{q}A'$ or $pe \rightarrow qq\bar{q}e$ can be used to measure the valence light-front wavefunction of the proton as well as its intrinsic heavy quark Fock states. Similarly, the hidden-color Fock states²⁸ of the six-quark deuteron, can be dissociated to final states such as $\Delta^{++}\Delta^{-}$.

4 Antishadowing of Nuclear Structure Functions

One of the novel features of QCD involving nuclei is the *antishadowing* of the nuclear structure functions which is observed in deep inelastic lepton scattering and other hard processes. Empirically, one finds $R_A(x, Q^2) \equiv (F_{2A}(x, Q^2)/(A/2)F_d(x, Q^2)) > 1$ in the domain $0.1 < x < 0.2$; *i.e.*, the measured nuclear structure function (referenced to the deuteron) is larger than the scattering on a set of A independent nucleons. The shadowing of the nuclear structure functions: $R_A(x, Q^2) < 1$ at small $x < 0.1$ can be readily understood in terms of the Gribov-Glauber theory. Consider the two-step process illustrated in Fig. 1 in the nuclear target rest frame. The incoming $q\bar{q}$ dipole first interacts diffractively $\gamma^*N_1 \rightarrow (q\bar{q})N_1$ on nucleon N_1 leaving it intact. This is the leading-twist diffractive deep inelastic scattering (DDIS) process which has been measured at HERA to constitute approximately 10% of the DIS cross section at high energies. The $q\bar{q}$ state then interacts inelastically on a downstream nucleon N_2 : $(q\bar{q})N_2 \rightarrow X$. The phase of the pomeron-dominated DDIS amplitude is close to imaginary, and the Glauber cut provides another phase i , so that the two-step process has opposite phase and destructively interferes with the one-step DIS process $\gamma^*N_2 \rightarrow X$ where N_1 acts as an unscattered spectator. The one-step and two step amplitudes can coherently interfere as long as the momentum transfer to the nucleon N_1 is sufficiently small that it remains in the nuclear target; *i.e.*, the Ioffe length²⁹ $L_I = 2M\nu/Q^2$ is large compared to the inter-nucleon separation. In effect, the flux reaching the interior nucleons is diminished, thus reducing the number of effective nucleons and $R_A(x, Q^2) < 1$.

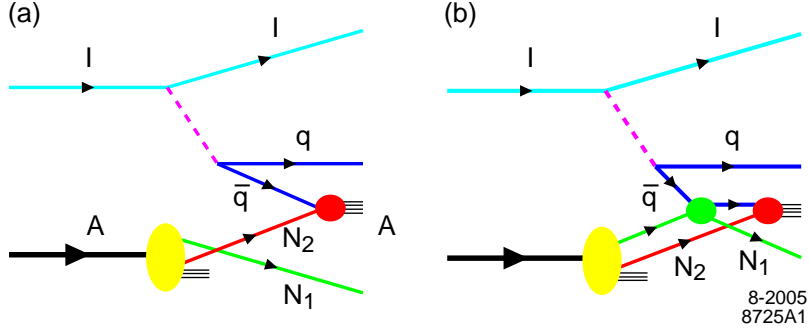


Figure 1: Illustration of one-step and two-step processes.

There are also leading-twist diffractive contributions $\gamma^* N_1 \rightarrow (q\bar{q})N_1$ arising from Reggeon exchanges in the t -channel.³⁰ For example, isospin-non-singlet $C = +$ Reggeons contribute to the difference of proton and neutron structure functions, giving the characteristic Kuti-Weisskopf $F_{2p} - F_{2n} \sim x^{1-\alpha_R(0)} \sim x^{0.5}$ behavior at small x . The x dependence of the structure functions reflects the Regge behavior $\nu^{\alpha_R(0)}$ of the virtual Compton amplitude at fixed Q^2 and $t = 0$. The phase of the diffractive amplitude is determined by analyticity and crossing to be proportional to $-1 + i$ for $\alpha_R = 0.5$, which together with the phase from the Glauber cut, leads to *constructive* interference of the diffractive and nondiffractive multi-step nuclear amplitudes. Furthermore, because of its x dependence, the nuclear structure function is enhanced precisely in the domain $0.1 < x < 0.2$ where antishadowing is empirically observed. The strength of the Reggeon amplitudes is fixed by the fits to the nucleon structure functions, so there is little model dependence.

As noted in Section 1, the Bjorken-scaling diffractive contribution to DIS arises from the rescattering of the struck quark after it is struck (in the parton model frame $q^+ \leq 0$), an effect induced by the Wilson line connecting the currents. Thus one cannot attribute DDIS to the physics of the target nucleon computed in isolation.⁴ Similarly, since shadowing and antishadowing arise from the physics of diffraction, we cannot attribute these phenomena to the structure of the nucleus itself: shadowing and antishadowing arise because of the $\gamma^* A$ collision and the history of the $q\bar{q}$ dipole as it propagates through the nucleus.

In a recent paper, Ivan Schmidt, Jian-Jun Yang, and I³¹ have extended this analysis to the shadowing and antishadowing of all of the electroweak structure functions. Quarks of different flavors will couple to different Reggeons; this leads to the remarkable prediction that nuclear antishadowing is not universal; it depends on the quantum numbers of the struck quark. This picture leads to substantially different antishadowing for charged and neutral current reactions, thus affecting the extraction of the weak-mixing angle θ_W . See Fig. 2. We find that part of the anomalous NuTeV result³² for θ_W could be due to the non-universality of nuclear antishadowing for charged and neutral currents. Detailed measurements of the nuclear dependence of individual quark structure functions are thus needed to establish the distinctive phenomenology of shadowing and antishadowing and to make the NuTeV results definitive. Schmidt, Yang, and I have also identified contributions to the nuclear multi-step reactions which arise from odderon exchange and also hidden color degrees of freedom in the nuclear wavefunction. There are other ways in which this new view of antishadowing can be tested; antishadowing can also depend on the target and beam polarization.

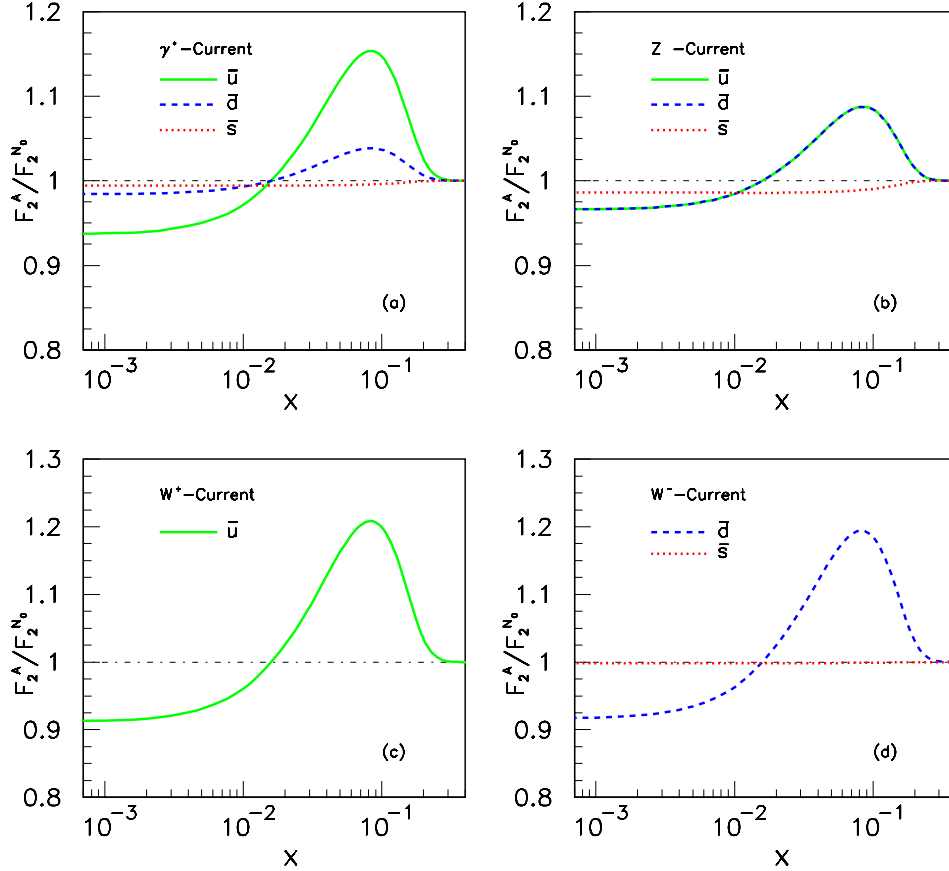


Figure 2: Model predictions³¹ for interactions of electroweak interactions on antiquarks in nuclear targets. The antishadowing effect is not as large for quark currents.

Acknowledgments

This talk is based on collaborations with Rikard Enberg, Paul Hoyer, Dae Sung Hwang, Gunnar Ingelman, Hung Jung Lu, Ivan Schmidt and Jian-Jun Yang. The work was supported in part by the Department of Energy, contract No. DE-AC02-76SF00515.

References

1. C. Adloff *et al.* [H1 Collaboration], Z. Phys. C **76**, 613 (1997) [arXiv:hep-ex/9708016].
2. J. Breitweg *et al.* [ZEUS Collaboration], Eur. Phys. J. C **6**, 43 (1999) [arXiv:hep-ex/9807010].
3. S. J. Brodsky, L. Frankfurt, J. F. Gunion, A. H. Mueller and M. Strikman, Phys. Rev. D **50**, 3134 (1994) [arXiv:hep-ph/9402283].
4. S. J. Brodsky, P. Hoyer, N. Marchal, S. Peigne and F. Sannino, Phys. Rev. D **65**, 114025 (2002) [arXiv:hep-ph/0104291].
5. A. V. Belitsky, X. Ji and F. Yuan, Nucl. Phys. B **656**, 165 (2003) [arXiv:hep-ph/0208038].
6. J. C. Collins and A. Metz, Phys. Rev. Lett. **93**, 252001 (2004) [arXiv:hep-ph/0408249].
7. J. C. Collins, Phys. Lett. B **536**, 43 (2002) [arXiv:hep-ph/0204004].
8. J. C. Collins, Acta Phys. Polon. B **34**, 3103 (2003) [arXiv:hep-ph/0304122].
9. S. J. Brodsky, R. Enberg, P. Hoyer and G. Ingelman, Phys. Rev. D **71**, 074020 (2005) [arXiv:hep-ph/0409119].

10. A. Edin, G. Ingelman and J. Rathsman, Phys. Lett. B **366**, 371 (1996) [arXiv:hep-ph/9508386].
11. S. J. Brodsky, D. S. Hwang and I. Schmidt, Phys. Lett. B **530**, 99 (2002) [arXiv:hep-ph/0201296].
12. M. Burkardt, Nucl. Phys. Proc. Suppl. **141**, 86 (2005) [arXiv:hep-ph/0408009].
13. A. Airapetian *et al.* [HERMES Collaboration], Phys. Rev. Lett. **94**, 012002 (2005) [arXiv:hep-ex/0408013].
14. H. Avakian and L. Elouadrhiri [CLAS Collaboration], AIP Conf. Proc. **698**, 612 (2004).
15. S. J. Brodsky, D. S. Hwang and I. Schmidt, Nucl. Phys. B **642**, 344 (2002) [arXiv:hep-ph/0206259].
16. D. Boer, S. J. Brodsky and D. S. Hwang, Phys. Rev. D **67**, 054003 (2003) [arXiv:hep-ph/0211110].
17. S. J. Brodsky, D. S. Hwang and I. Schmidt, Phys. Lett. B **553**, 223 (2003) [arXiv:hep-ph/0211212].
18. S. J. Brodsky and A. H. Mueller, Phys. Lett. B **206**, 685 (1988).
19. G. Bertsch, S. J. Brodsky, A. S. Goldhaber and J. F. Gunion, Phys. Rev. Lett. **47**, 297 (1981).
20. L. Frankfurt, G. A. Miller and M. Strikman, Found. Phys. **30**, 533 (2000) [arXiv:hep-ph/9907214].
21. N. N. Nikolaev, W. Schafer and G. Schwiete, Phys. Rev. D **63**, 014020 (2001) [arXiv:hep-ph/0009038].
22. E. M. Aitala *et al.* [E791 Collaboration], Phys. Rev. Lett. **86**, 4773 (2001) [arXiv:hep-ex/0010044].
23. G. P. Lepage and S. J. Brodsky, Phys. Lett. B **87**, 359 (1979).
24. A. V. Efremov and A. V. Radyushkin, Theor. Math. Phys. **42**, 97 (1980) [Teor. Mat. Fiz. **42**, 147 (1980)].
25. G. P. Lepage and S. J. Brodsky, Phys. Rev. D **22**, 2157 (1980).
26. E. M. Aitala *et al.* [E791 Collaboration], Phys. Rev. Lett. **86**, 4768 (2001) [arXiv:hep-ex/0010043].
27. S. J. Brodsky and G. F. de Teramond, Phys. Lett. B **582**, 211 (2004) [arXiv:hep-th/0310227].
28. S. J. Brodsky, C. R. Ji and G. P. Lepage, Phys. Rev. Lett. **51**, 83 (1983).
29. B. L. Ioffe, Phys. Lett. B **30**, 123 (1969).
30. S. J. Brodsky and H. J. Lu, Phys. Rev. Lett. **64**, 1342 (1990).
31. S. J. Brodsky, I. Schmidt and J. J. Yang, Phys. Rev. D **70**, 116003 (2004) [arXiv:hep-ph/0409279].
32. G. P. Zeller *et al.* [NuTeV Collaboration], Phys. Rev. Lett. **88**, 091802 (2002) [Erratum-*ibid.* **90**, 239902 (2003)] [arXiv:hep-ex/0110059].